

# Image Cover Sheet

<b>CLASSIFICATION</b>  UNCLASSIFIED	<b>SYSTEM NUMBER</b> 149065 
---	--

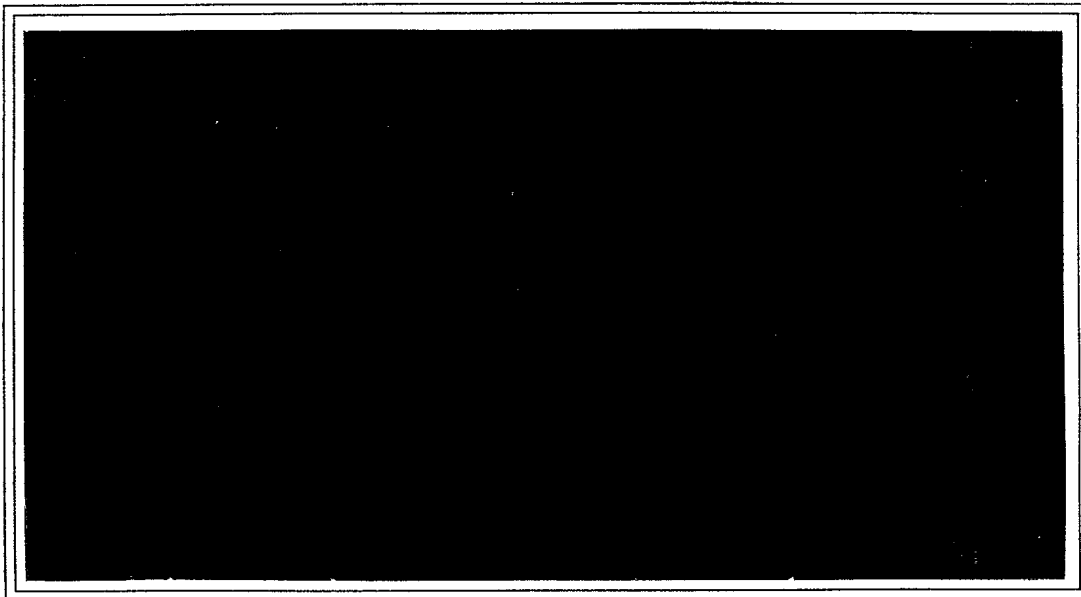
**TITLE**  
PROBABILITY POINTS FOR THE KURTOSIS OF A NORMAL SAMPLE WITH KNOWN MEAN

**System Number:**  
**Patron Number:**  
**Requester:**

**Notes:**

**DSIS Use only:**  
**Deliver to:** FF





**DEFENCE RESEARCH ESTABLISHMENT PACIFIC**

Research and Development Branch

Department of National Defence

**Canada**



## DEFENCE RESEARCH ESTABLISHMENT PACIFIC

---

CFB Esquimalt, FMO Victoria, B.C. V0S 1B0

Technical Memorandum 94-143

### PROBABILITY POINTS FOR THE KURTOSIS OF A NORMAL SAMPLE WITH KNOWN MEAN

by

Brian H. Maranda

November 1994



Approved By:



Chief DREP

Research and Development Branch  
Department of National Defence



### ABSTRACT

Probability points are computed for the sample kurtosis of independent, identically distributed Gaussian variates when the sample moments are taken about the true mean. The method of computation allows the accurate determination of the probability points even for small tail probabilities, and values are tabulated for probabilities as small as  $10^{-4}$ . Moreover, the results suggest that the probability points tabulated here may also be used when the sample moments are taken about the sample mean.

### RÉSUMÉ

On calcul les points qui donnent des probabilités spécifiées pour le kurtosis d'un échantillon de variables aléatoires gaussiennes, indépendantes et distribuées identiquement. Les moments de l'échantillon sont calculés autour de la vraie moyenne. La méthode de calcul permet la détermination précise des points de probabilité même si les probabilités sont petites, et un tableau est présenté pour des probabilités aussi petites que  $10^{-4}$ . Les résultats suggèrent d'ailleurs que les points de probabilité tabulés ici peuvent être également utilisés quand on prend la moyenne de l'échantillon comme centre des moments de l'échantillon.



## 1. INTRODUCTION

Given a random variable  $X$  with probability density function  $p_X(\cdot)$ , the  $k$ th moment about zero and about the mean are respectively defined by

$$\mu'_k = \int_{\mathbb{R}} x^k p_X(x) dx \quad \text{and} \quad \mu_k = \int_{\mathbb{R}} (x - \mu'_1)^k p_X(x) dx,$$

where the support of  $X$  is assumed to be the real line,  $\mathbb{R}$ . The kurtosis of  $X$  is defined by  $\beta_2 = \mu_4/\mu_2^2$ , and is equal to 3 when the distribution is normal. Given a sample of  $N$  independent observations  $X_n$  from a population with density  $p_X$ , the  $k$ th sample moment about zero and about the sample mean are defined by

$$m'_k = \frac{1}{N} \sum_{n=1}^N X_n^k \quad \text{and} \quad m_k = \frac{1}{N} \sum_{n=1}^N (X_n - m'_1)^k.$$

The sample kurtosis is then given by  $b_2 = m_4/m_2^2$ . For a normal population the sample kurtosis is approximately 3, and its deviation from 3 is an indication of whether the parent population is indeed Gaussian. In signal processing applications, the sample kurtosis may be computed and compared with a threshold  $\alpha$  for hundreds or even thousands of independent data blocks (e.g., to locate spikes in Gaussian noise). In such applications the probability  $\Pr(b_2 > \alpha)$  for Gaussian data alone must be kept small, typically  $10^{-3}$  to  $10^{-4}$ , in order to prevent an excessive number of false alarms.

In a series of papers<sup>1-3</sup>, Pearson considered the computation of the probability points for the sample kurtosis, i.e., points  $\alpha$  that yield a desired value of the tail probability  $\Pr(b_2 > \alpha)$ . The calculation of probability points for  $b_2$  is difficult, because the exact sampling density is not known for arbitrary  $N$ . Pearson's approach was to approximate the unknown density by a standard parametric form, matching the first several moments to determine the parameters. This standard form was then numerically integrated to find the probability points. This approach is of limited accuracy, particularly for small probabilities that require knowledge of the far tails of the density function, and for this reason Pearson limited himself to tail probabilities of 0.05 and 0.01. The accuracy is also limited for small  $N$ , and in this case Monte Carlo techniques have been used.<sup>4,5</sup>

In this paper, probability points are computed for the sample kurtosis when the sample moments are computed about the true mean  $\mu'_1$ . Since we can define new random variables centred about the mean, it may be assumed without loss of generality that  $\mu'_1 = 0$ , and we work with  $b'_2 \equiv m'_4/(m'_2)^2$ . Unlike the case of  $b_2$ , no approximations need be made in the analysis of  $b'_2$ , and only numerical processes limit the number of decimal places that can be obtained in the computation of the probability points. Although

the assumption that the mean is known is made primarily for reasons of computational tractability, it can be justified in two ways. First of all, in many physical applications  $\mu'_1$  can be considered known *a priori*. For example, consider the recording of underwater acoustic noise using a pressure transducer followed by an amplifier. The amplifier will typically have no DC response, and any DC offset at its output will be accurately known. Since the system has no DC response, this offset can be taken as the true mean of the measured pressure data. Secondly, the evidence suggests that the probability points for  $b_2$  are very close to those for  $b'_2$ . More will be said about this later.

## 2. METHOD OF COMPUTATION

### 2.1 Introduction

Throughout the paper,  $Q(\alpha)$  will denote the tail probability  $\Pr(b'_2 > \alpha)$ . We define a vector  $\mathbf{s} = (s_1, s_2)$ , where  $s_1 = \sum X_n^4$  and  $s_2 = \sum X_n^2$ , and denote by  $p_{\mathbf{s}}$  the probability density function of  $\mathbf{s}$ . For convenience in the subsequent derivation, the sums  $s_1$  and  $s_2$  have not been normalized by  $N$ . Then  $b'_2 = Ns_1/s_2^2$ , and the desired tail probability is given by  $Q(\alpha) = \Pr(s_1 - \tilde{\alpha}s_2^2 > 0)$ , where  $\tilde{\alpha} \equiv \alpha/N$  is a normalized probability point. Setting  $\mathbf{u} = (u_1, u_2)$ , the tail probability is given in integral form by

$$Q(\alpha) = \int_{u_1 - \tilde{\alpha}u_2^2 > 0} p_{\mathbf{s}}(\mathbf{u}) d\mathbf{u} = \int_0^{\infty} \left\{ \int_{\tilde{\alpha}u_2^2}^{\infty} p_{\mathbf{s}}(u_1, u_2) du_1 \right\} du_2, \quad (1)$$

where in the last step the two-dimensional integral has been written as two iterated integrals. For future reference we note that the derivative of  $Q(\alpha)$  with respect to  $\alpha$  is given by

$$Q'(\alpha) = -\frac{1}{N} \int_0^{\infty} p_{\mathbf{s}}(\tilde{\alpha}u_2^2, u_2) u_2^2 du_2. \quad (2)$$

The rest of the paper will be devoted to the computation of specified probability points via the numerical integration of Eq. (1). The difficulty here is that the density function  $p_{\mathbf{s}}$  does not appear to be expressible in terms of standard functions. We shall perform numerically the Fourier inversion of the characteristic function of  $\mathbf{s}$ , and so now turn to a consideration of this function.

### 2.2 The characteristic function

The joint characteristic function  $\phi_{\mathbf{s}}(\mathbf{t})$  of  $\mathbf{s}$  is given by  $\phi_{\mathbf{s}}(\mathbf{t}) = E\{e^{i\langle \mathbf{t}, \mathbf{s} \rangle}\}$ , where  $\mathbf{t} = (t_1, t_2)$  and  $\langle \mathbf{t}, \mathbf{s} \rangle$  is the vector inner product. As the  $X_n$  are independent and identically distributed with a normal distribution, we have

$$\phi_{\mathbf{s}}(\mathbf{t}) = \frac{1}{(2\pi\sigma^2)^{N/2}} \int_{\mathbb{R}^N} e^{i\langle \mathbf{t}, \mathbf{s} \rangle} \prod_{n=1}^N e^{-x_n^2/2\sigma^2} dx_1 \cdots dx_N. \quad (3)$$

Since  $b'_2$  is invariant to scale changes, we shall take  $\sigma = 1$  in what follows. It easily follows from Eq. (3) that  $\phi_s(\mathbf{t}) = \phi(\mathbf{t})^N$ , where

$$\phi(\mathbf{t}) = \frac{1}{\sqrt{2\pi}} \int_{\mathbb{R}} \exp\{it_1x^4 - \frac{1}{2}(1 - 2it_2)x^2\} dx \quad (4)$$

is the joint characteristic function of any pair  $(X_n^4, X_n^2)$ . The convenient decomposition  $\phi_s(\mathbf{t}) = \phi(\mathbf{t})^N$  is made possible by taking the sample moments about the true mean; when the moments are taken about the sample mean, such a decomposition does not occur. In the Appendix it is shown that

$$\phi(\mathbf{t}) = (1 - 2it_2)^{-\frac{1}{2}} \left(\frac{\pi\zeta}{2}\right)^{\frac{1}{2}} e^{i(\zeta - 3\pi/8)} H_{\frac{1}{4}}^{(2)}(\zeta), \quad (5)$$

where  $H_{\frac{1}{4}}^{(2)}(\cdot)$  is the Hankel function of the second kind and order  $\frac{1}{4}$ , and  $\zeta \equiv (1 - 2it_2)^2 / (32t_1)$ . Since  $\zeta$  is in general complex-valued, consideration must be given to the domain of definition of the functions in Eq. (5). When the square root and the Hankel function have their principal values, formula (5) is used for  $\mathbf{t}$  in the open right-half plane. The reflection formula  $\phi(-\mathbf{t}) = \phi^*(\mathbf{t})$ , where the asterisk denotes complex conjugation, is then used to compute the characteristic function in the left-half plane. This leaves only the line  $t_1 = 0$  (the  $t_2$ -axis) for which the characteristic function has not been defined, but from Eq. (4) it follows that  $\phi(0, t_2) = (1 - 2it_2)^{-\frac{1}{2}}$ . This last equation is, of course, the characteristic function for a  $\chi_1^2$  variate, since when  $t_1 = 0$  we are left with the square of a Gaussian random variable.

Expansions of the Hankel function can be used to examine the behaviour of the characteristic function in certain parts of the  $\mathbf{t}$ -plane. When  $|\zeta| \gg 1$ , the asymptotic expansion of the Hankel function for large argument<sup>6</sup> leads to the simple result

$$\phi(\mathbf{t}) \sim (1 - 2it_2)^{-\frac{1}{2}} \sum_{m=0}^{\infty} \frac{(\frac{1}{4}, m)}{(2i\zeta)^m} = (1 - 2it_2)^{-\frac{1}{2}} \left(1 - \frac{3}{32i\zeta} + \dots\right), \quad (6)$$

where  $(\nu, 0) \equiv 0$  and  $(\nu, m) \equiv (4\nu^2 - 1) \dots [4\nu^2 - (2m - 1)^2] / 2^{2m} m!$  for  $m \geq 1$ . From the definition of  $\zeta$  it follows that  $|\zeta| \rightarrow \infty$  as  $t_1 \rightarrow 0+$  for a fixed  $t_2$ , and hence from Eq. (6) we see that as  $t_1 \rightarrow 0+$  the characteristic function approaches its value on the  $t_2$  axis,  $\phi(0, t_2) = (1 - 2it_2)^{-\frac{1}{2}}$ , as expected. The same behaviour obtains for a fixed  $t_1$  when  $t_2 \rightarrow \pm\infty$ . On the other hand, when  $t_1 \rightarrow \infty$  so that  $\zeta$  is small, the asymptotic form of the Hankel function for small argument (see entry 9.1.9 of Ref. 7) yields

$$\phi(\mathbf{t}) \sim \frac{1}{2\sqrt{2\pi}} \Gamma(\frac{1}{4}) e^{i\pi/8} t_1^{-1/4},$$

where  $\Gamma(\cdot)$  is the Gamma function. Note the slow decay of the characteristic function at infinity in the  $\mathbf{t}$ -plane. This slow decay would make numerical work very difficult, but fortunately we are interested in  $\phi_{\mathbf{s}}(\mathbf{t}) = \phi(\mathbf{t})^N$ , which has a substantial rate of decay even for moderate values of  $N$ . This decay allowed the truncation of integrals over an infinite range to a finite interval in the subsequent numerical work.

Except for some regions where Eq. (6) was used, the characteristic function was evaluated in the right-half  $\mathbf{t}$ -plane directly from Eq. (5). A NAG routine<sup>8</sup> was used to compute the scaled Hankel function  $e^{i\zeta} H_{\frac{1}{4}}^{(2)}(\zeta)$  in Eq. (5).

### 2.3 Numerical procedure for computing $Q(\alpha)$

The probability density function  $p_{\mathbf{s}}$  is given by Fourier inversion of the characteristic function  $\phi_{\mathbf{s}}$ :

$$p_{\mathbf{s}}(\mathbf{u}) = \frac{1}{(2\pi)^2} \int_{\mathbb{R}^2} \phi_{\mathbf{s}}(\mathbf{t}) e^{-i\langle \mathbf{t}, \mathbf{u} \rangle} d\mathbf{t} = \frac{1}{(2\pi)^2} \int_{\mathbb{R}^2} \phi(\mathbf{t})^N e^{-i\langle \mathbf{t}, \mathbf{u} \rangle} d\mathbf{t}. \quad (7)$$

There appears to be little hope of performing the integration analytically. An approximate method would be to find an asymptotic expression for the integral (7), but it is not clear that the long tails of the distribution, resulting from the fourth moment in the kurtosis, can be represented accurately in this way. For this reason, a purely numerical approach was adopted. The direct substitution of Eq. (7) into Eq. (1) yields a four-fold integral to be evaluated numerically, but it is possible to reduce the procedure to the numerical integration of a three-fold integral as follows. First we introduce the function

$$\psi_{\mathbf{s}}(t_1, u_2) = \frac{1}{2\pi} \int_{\mathbb{R}} \phi_{\mathbf{s}}(\mathbf{t}) e^{-it_2 u_2} du_2, \quad (8)$$

which results from performing one of the integrations in Eq. (7). Using a result derived by Nuttall<sup>9</sup>, we can write, for any positive  $u_2$  and  $a$ ,

$$\int_a^\infty p_{\mathbf{s}}(u_1, u_2) du_1 = \frac{2}{\pi} \int_0^\infty \text{Im}\{\psi_{\mathbf{s}}(t_1, u_2)\} \frac{\cos at_1}{t_1} dt_1. \quad (9)$$

Taking  $a = \tilde{\alpha}u_2^2$  in this equation directly yields the inner integral in the iterated integral of Eq. (1). Hence, it is not necessary to compute  $p_{\mathbf{s}}(\mathbf{u})$  explicitly as in Eq. (7), and in this manner one integration is eliminated. Finally, the outer integral in Eq. (1) must also be computed via numerical integration, for a total of three nested quadratures.

An overview of the numerical procedure for computing  $Q(\alpha)$  is now given. The first step is to compute  $\psi_{\mathbf{s}}(t_1, u_2)$  by the numerical integration of Eq. (8) using the fast Fourier transform (FFT). The use of the FFT is equivalent to a trapezoidal rule; see

Ref. 10 for a discussion of this method. The advantage of the FFT is that, for a given  $t_1$ , it allows the efficient computation of  $\psi_s(t_1, u_2)$  on an equi-spaced grid of  $u_2$  values in a single calculation. By discretizing  $t_1$ , the result is  $\psi_s(t_1, u_2)$  evaluated on a rectangular grid. Next, integral (9) is evaluated numerically for each value of  $u_2$  on the grid via the trapezoidal rule. The fast Fourier transform is not used in this case because the value of the integral is desired only at one point, namely  $a = \bar{\alpha}u_2^2$ . Lastly, the outer integral in Eq. (1) is evaluated using a high-order quadrature rule, a compounded 7-point Newton-Cotes formula.

The integrand on the right-hand side of Eq. (9) is not defined at  $t_1 = 0$ , but its limit exists for  $t_1 \rightarrow 0+$ . It is easy to show that, for arbitrary  $u_2$ ,

$$\lim_{t_1 \rightarrow 0+} \text{Im}\{\psi_s(t_1, u_2)\} \frac{\cos at_1}{t_1} = \text{Im} \left\{ \frac{\partial \psi_s}{\partial t_1}(0, u_2) \right\}, \quad (10)$$

and from Eq. (8) it immediately follows that

$$\frac{\partial \psi_s}{\partial t_1}(0, u_2) = \frac{1}{2\pi} \int_{\mathbb{R}} \frac{\partial \phi_s}{\partial t_1}(0, t_2) e^{-it_2 u_2} dt_2. \quad (11)$$

Some analysis gives the simple result  $\partial \phi_s(0, t_2)/\partial t_1 = 3iN(1 - 2it_2)^{-\frac{1}{2}(N+4)}$ , whence it follows that the partial derivative of  $\psi_s$  required in Eq. (10) is expressible in terms of the density function of a  $\chi_{N+4}^2$  variate. Thus: when  $t_1 > 0$ , the function  $\psi_s(t_1, u_2)$  is computed by FFT quadrature of Eq. (8) and is substituted directly into the integrand of Eq. (9). When  $t_1 = 0$ , the integrand in Eq. (9) is replaced by the right-hand side of Eq. (10), which is evaluated from a chi-squared density function.

## 2.4 Finding the probability points

The final step in the numerical procedure is to compute the probability point,  $\alpha$ , for an assigned value of  $Q(\alpha)$ . This is a problem in root-finding, and Newton's method was employed. The derivative required for Newton's method was computed by numerical quadrature of Eq. (2); this numerical quadrature is somewhat simpler than that described for Eq. (1), and can be performed simultaneously with it. The expected rapid convergence of Newton's method was obtained in practice, and at most 15 iterations were required in all cases.

The development so far has been for the upper tail  $Q(\alpha) = \Pr(b'_2 > \alpha)$ , but probability points on the lower tail were computed as well. If  $P(\alpha) \equiv \Pr(b'_2 < \alpha)$ , then  $P(\alpha) = 1 - Q(\alpha)$ , but this last relation is inadequate for numerical work due to the high accuracy that would be required in the values of  $Q(\alpha)$  when  $P(\alpha)$  is small. For this

reason a separate code was written to compute  $P(\alpha)$  directly by modifying the integrand of Eq. (9); see Eq. (5) in Ref. 9.

### 3. NUMERICAL RESULTS

#### 3.1 Tables of probability points

Probability points were computed by the above procedure on a VAX 9000 computer using double-precision (16 decimal digit) arithmetic. Table I provides the computed probability points of  $b'_2$  for the lower tail, and Table II for the upper tail. The values in the tables have been rounded to 5 figures; the following subsections give some details on the accuracy of the computations.

Since  $m'_1 \rightarrow \mu'_1$  almost surely as  $N \rightarrow \infty$ , it is expected that the probability points of  $b_2$  and  $b'_2$  will become close together as  $N$  grows large. What is remarkable is the apparent speed with which this coalescence takes place. A comparison can be made with Table 34 of the Biometrika Tables<sup>11</sup>, which provides probability points for  $b_2$  to three significant figures for probabilities 0.05 and 0.01. When the values tabulated here are rounded to three figures, the agreement is good to all three figures at the 5% level and usually within one unit in the last place at the 1% level. It may be conjectured that, save perhaps for the smallest probabilities, the probability points tabulated here for  $b'_2$  will agree with those for  $b_2$  to several decimal places.

#### 3.2 Accuracy in computing the tail probability

Apart from round-off error, the errors in the numerical computation come primarily from two sources: from the truncation of the infinite integrals to finite intervals of integration, and from the application of quadrature rules to the truncated integrals. The truncation limits were set by examining contour plots of  $|\phi_s(\mathbf{t})|$  in the  $\mathbf{t}$ -plane. The significant region of integration is near the origin, where  $|\phi_s(\mathbf{t})| \simeq 1$ , and the integrals were truncated at a point where  $|\phi_s(\mathbf{t})|$  had fallen below  $10^{-16}$ . The quadrature errors were handled by doubling the number of points in the quadrature rules until the result converged. The result generally stabilized to 9 or 10 decimal digits, suggesting that the least significant 6 or 7 digits were affected by round-off. As a check, some of the tail probabilities were re-calculated using quadruple-precision arithmetic (32 decimal digits) in the numerical integrations, although the Hankel function in Eq. (5) was still computed using the double-precision NAG routine. The results generally agreed to 9 or 10 decimal places, as expected. Moreover, a check was made in selected cases by doubling the truncation limits and verifying that the computed values did not change significantly.

It should be pointed out that the smaller values of  $N$  required many more points in the quadrature rules to obtain an accurate result. For example, when  $N = 50$  the

Table I. Points  $\alpha$  for specified values of  $P(\alpha) = \Pr(b'_2 < \alpha)$ 

$N$	Probability $P(\alpha)$					
	0.05	0.01	0.005	0.001	0.0005	0.0001
50	2.1479	1.9699	1.9128	1.8061	1.7681	1.6929
100	2.3469	2.1877	2.1354	2.0359	2.0000	1.9279
150	2.4464	2.3008	2.2523	2.1594	2.1256	2.0571
200	2.5095	2.3741	2.3286	2.2410	2.2090	2.1438
300	2.5883	2.4676	2.4266	2.3470	2.3177	2.2577
400	2.6374	2.5270	2.4893	2.4156	2.3883	2.3323
500	2.6720	2.5694	2.5341	2.4650	2.4393	2.3864
600	2.6980	2.6016	2.5683	2.5030	2.4786	2.4282
700	2.7186	2.6272	2.5956	2.5333	2.5101	2.4619
800	2.7353	2.6483	2.6181	2.5584	2.5361	2.4899
900	2.7494	2.6660	2.6370	2.5797	2.5581	2.5136
1000	2.7613	2.6812	2.6533	2.5979	2.5771	2.5340
1250	2.7850	2.7114	2.6856	2.6344	2.6152	2.5750
1500	2.8027	2.7341	2.7101	2.6621	2.6440	2.6063

Table II. Points  $\alpha$  for specified values of  $Q(\alpha) = \Pr(b'_2 > \alpha)$ 

$N$	Probability $Q(\alpha)$					
	0.05	0.01	0.005	0.001	0.0005	0.0001
50	3.9908	4.8817	5.3033	6.3812	6.8874	8.1495
100	3.7727	4.3824	4.6649	5.3848	5.7257	6.5930
150	3.6518	4.1283	4.3445	4.8894	5.1461	5.8001
200	3.5733	3.9708	4.1484	4.5904	4.7971	5.3226
300	3.4747	3.7813	3.9149	4.2409	4.3911	4.7701
400	3.4135	3.6682	3.7772	4.0390	4.1581	4.4559
500	3.3709	3.5915	3.6846	3.9054	4.0048	4.2511
600	3.3390	3.5353	3.6172	3.8095	3.8952	4.1059
700	3.3141	3.4920	3.5656	3.7368	3.8124	3.9970
800	3.2939	3.4573	3.5244	3.6794	3.7473	3.9120
900	3.2771	3.4288	3.4907	3.6327	3.6946	3.8435
1000	3.2628	3.4049	3.4625	3.5939	3.6508	3.7870
1250	3.2349	3.3585	3.4081	3.5199	3.5677	3.6808
1500	3.2142	3.3248	3.3687	3.4669	3.5085	3.6060

characteristic function  $\phi(t)$  had to be evaluated at approximately 16 million points; in contrast, for  $N = 500$  the required number of function evaluations was reduced by a factor of 32. Thus the computations were much more rapid for the larger sample sizes.

### 3.3 Sensitivity of the tail probability to perturbations in $\alpha$

We define the error amplification of a function  $f$  at  $x$  by  $A(f; x) = x f'(x)/f(x)$ . Letting  $\delta_f(x)$  be the relative error in  $f(x)$  caused by a relative error  $\delta$  in  $x$ , it may easily be shown from the Taylor expansion of  $f(x(1+\delta))$  about  $x$  that  $\delta_f(x) \cong A(f; x) \delta$ . Hence if  $|A(f; x)| > 1$ , the relative error in  $x$  is amplified in computing  $f(x)$ ; if  $|A(f; x)| < 1$ , the relative error is damped. In the case at hand, we of course take  $f$  to be either  $P(\alpha)$  or  $Q(\alpha)$ . Since the derivative was already computed in order to use Newton's method, the error amplification could be evaluated with negligible effort. In all cases it was found that the error amplification exceeded unity, meaning that 5 decimal places in  $\alpha$  corresponds to fewer than 5 decimal places in the tail probability. Since the tail probabilities were computed to 9 or 10 decimal places, the values of  $\alpha$  tabulated in Tables I and II should be correct to the number of decimals given.

In general, the sensitivity to perturbations in  $\alpha$  increases as  $N$  increases. The error amplification resulting from the steepness of the lower tail can be severe, approaching 120 in the case  $N = 1500$  and  $P(\alpha) = 0.0001$ . The error amplification for the upper tail is less severe, usually being in the range 10–50 in absolute value.

## 4. SUMMARY

In this paper, a numerical method was developed for computing probability points for the sample kurtosis of independent and identically distributed Gaussian variates. The method makes no approximations and allows the determination of the probability points for small values of the tail probability. However, it was assumed that the true mean of the input data is known and that the sample moments are computed about this mean. In practice, the true mean is unknown and must be estimated by the sample mean. However, comparison with published tables for probabilities 0.05 and 0.01 suggests that the probability points are little affected by the choice of center (true mean or sample mean) when computing the sample kurtosis, even for sample sizes as small as 50.

## APPENDIX

In this Appendix, Eq. (5) for the joint characteristic function  $\phi(t)$  is examined. We start with the function

$$\phi_{x^4}(z) = \left(\frac{2}{\pi}\right)^{\frac{1}{2}} \int_0^{\infty} \exp(-\frac{1}{2}x^2 + izx^4) dx, \quad (\text{A1})$$

which is the characteristic function of the fourth power of a standardized Gaussian variate. When  $z$  is complex, the integral (A1) exists for  $\text{Im}(z) \geq 0$  and defines an analytic function of  $z$  in  $\text{Im}(z) > 0$ . It follows from a result derived in Ref. 12 that  $\phi_{x^4}(z)$  has a Laurent expansion in powers of  $z^{\frac{1}{4}}$  that is convergent for  $|z| > 0$ . Thus  $\phi_{x^4}(z)$  can be continued analytically onto a four-sheeted Riemann surface, and has a branch point at the origin. The principal branch of  $\phi_{x^4}(z)$  is taken to be the branch in  $|\arg z| < \pi$  that is real-valued on the upper imaginary axis. The principal branch of  $\phi_{x^4}(z)$  then agrees with the value of the integral in Eq. (A1) in  $0 < \arg z < \pi$ . Another expression for  $\phi_{x^4}(z)$  is given by<sup>13</sup>

$$\phi_{x^4}(z) = \left(\frac{\pi\beta}{2}\right)^{\frac{1}{2}} e^{i(\beta-3\pi/8)} H_{\frac{1}{4}}^{(2)}(\beta), \quad (\text{A2})$$

where  $H_{\frac{1}{4}}^{(2)}(\cdot)$  is a Hankel function and  $\beta = (32z)^{-1}$ . This equation holds on the whole Riemann surface, excluding the branch point at  $z = 0$ . For computational purposes, however, it is desirable that the square root and Hankel functions in Eq. (A2) should have their principal values, as these are usually what is available in existing software packages. It can be shown that if the principal branches of these functions are chosen, then formula (A2) will assign  $\phi_{x^4}(z)$  its principal value. (Note that if  $|\arg z| < \pi$ , then  $|\arg \beta| < \pi$  as well.)

Now, the joint characteristic function in Eq. (5) is

$$\phi(\mathbf{t}) = \left(\frac{2}{\pi}\right)^{\frac{1}{2}} \int_0^\infty \exp(-\frac{1}{2}\omega x^2 + it_1 x^4) dx, \quad (\text{A3})$$

where  $\omega \equiv 1 - 2it_2$ . It is desired to transform the integral (A3) into the form of integral (A1) in order that formula (A2) may be applied. Although  $\omega$  is complex, we temporarily assume that  $\omega$  is real and positive; analytic continuation will later be used to extend the results back into the complex domain. With the change of variable  $y = \omega^{\frac{1}{2}}x$ , it follows from Eq. (A1) that

$$\begin{aligned} \left(\frac{2}{\pi}\right)^{\frac{1}{2}} \int_0^\infty \exp(-\frac{1}{2}\omega x^2 + it_1 x^4) dx &= \omega^{-\frac{1}{2}} \left(\frac{2}{\pi}\right)^{\frac{1}{2}} \int_0^\infty \exp(-\frac{1}{2}y^2 + it_1 \omega^{-2} y^4) dy, \\ &= \omega^{-\frac{1}{2}} \phi_{x^4}(t_1 \omega^{-2}). \end{aligned} \quad (\text{A4})$$

This holds for  $\omega$  real and positive. However, the integral on the left-hand side of Eq. (A4) defines an analytic function of  $\omega$  in  $\text{Re}(\omega) > 0$ , and  $\omega^{-\frac{1}{2}} \phi_{x^4}(t_1 \omega^{-2})$  is a (multi-valued) analytic function in the complex  $\omega$ -plane. It thus follows that  $\phi(\mathbf{t}) = \omega^{-\frac{1}{2}} \phi_{x^4}(t_1 \omega^{-2})$ , with the appropriate choice of branch on the right-hand side. For the rest of discussion,

we restrict  $\omega$  to the values  $\omega = 1 - 2it_2$  for  $t_2 \in \mathbb{R}$ , as required for computing  $\phi(\mathbf{t})$ . From the derivation of Eq. (A4) it is seen that  $\omega^{-\frac{1}{2}}$  should be real when  $\omega$  is real, and so the principal branch of  $\omega^{-\frac{1}{2}}$  may be used. In addition, it is found that  $|\arg(t_1\omega^{-2})| < \pi$  for  $t_1 > 0$ , and so the principal branch of  $\phi_{x^4}(t_1\omega^{-2})$  may be used when  $t_1 > 0$ . On the other hand,  $0 < \arg(t_1\omega^{-2}) < 2\pi$  for  $t_1 < 0$ . Thus in numerical computations, where the principal branch is desired, the formula  $\phi(\mathbf{t}) = \omega^{-\frac{1}{2}}\phi_{x^4}(t_1\omega^{-2})$  is used only for  $t_1 > 0$ , the reflection formula  $\phi(-\mathbf{t}) = \phi^*(\mathbf{t})$  being used when  $t_1 < 0$ . The case  $t_1 = 0$  represents a special case; since  $\phi_{x^4}(0) = 1$ , it follows that  $\phi(0, t_2) = \omega^{-\frac{1}{2}} = (1 - 2it_2)^{-\frac{1}{2}}$ .

Finally, when  $t_1 > 0$  and  $\phi_{x^4}(t_1\omega^{-2})$  has its principal value, formula (A2) may be used to write

$$\phi(\mathbf{t}) = \omega^{-\frac{1}{2}} \left( \frac{\pi\zeta}{2} \right)^{\frac{1}{2}} e^{i(\zeta-3\pi/8)} H_{\frac{1}{4}}^{(2)}(\zeta),$$

where  $\zeta = \omega^2/(32t_1) = (1 - 2it_2)^2/(32t_1)$ , and the square root and the Hankel function have their principal values. This is just Eq. (5) of the paper.

## REFERENCES

1. E.S. Pearson, "A further development of tests for normality," *Biometrika* **22**, 239–249 (1930).
2. E.S. Pearson, "Some problems arising in approximating to probability distributions, using moments," *Biometrika* **50**, 95–111 (1963).
3. E.S. Pearson, "Tables of percentage points of  $\sqrt{b_1}$  and  $b_2$  in normal samples; a rounding off," *Biometrika* **52**, 282–285 (1965).
4. T.S. Ferguson, "On the rejection of outliers," in *Proc. Fourth Berkeley Symp. on Math. Stat. and Prob.* **1**, 253–287 (1961).
5. R.B. D'Agostino and G.L. Tietjen, "Simulation probability points of  $b_2$  for small samples," *Biometrika* **58**, 669–672 (1971).
6. G.N. Watson, *A Treatise on the Theory of Bessel Functions*, 2nd ed. Cambridge: Cambridge University Press, 1966. Sec. 7.2.
7. M. Abramowitz and I.A. Stegun (eds.) *Handbook of Mathematical Functions*. New York: Dover Publications, 1965.
8. Fortran Library Mark 14, Numerical Algorithms Group, 1400 Opus Place, Downers Grove, IL.
9. A.H. Nuttall, "Alternate forms for numerical evaluation of cumulative probability distributions directly from characteristic functions," *Proc. IEEE* **58**, 1872–1873 (1970).

10. J.W. Cooley, P.A. Lewis, and P.D. Welch, "Application of the fast Fourier transform to computation of Fourier integrals, Fourier series, and convolution integrals," *IEEE Trans. Audio and Electroacoustics* **15**, 79–84 (1967).
11. E.S. Pearson and H.O. Hartley (eds.) *Biometrika Tables for Statisticians*, **1**. Cambridge: Cambridge University Press, 1966.
12. J.A. Fawcett and B.H. Maranda, "The optimal power law for the detection of a Gaussian burst in a background of Gaussian noise," *IEEE Trans. Inform. Theory* **37**, 209–214 (1991).
13. B.H. Maranda and J.A. Fawcett, "The performance analysis of a fourth-moment detector," in *Proc. IEEE Int. Conf. on Acoust., Speech, and Signal Proc.*, **3**, 1357–1360 (1990).

## DISTRIBUTION

REPORT NUMBER: Technical Memorandum 94-143  
TITLE: Probability Points for the Kurtosis of a  
Normal Sample with Known Mean  
AUTHOR: Brian H. Maranda  
DATED: November 1994

1 - DSIS  
1 - DRDM  
1 - DMOR  
2 - DREA  
10 - DREP

<b>DOCUMENT CONTROL DATA</b>		
(Security classification of title, body of abstract and indexing annotation must be entered when the overall document is classified)		
1. ORIGINATOR (the name and address of the organization preparing the document. Organizations for whom the document was prepared, e.g. Establishment sponsoring a contractor's report, or tasking agency, are entered in section 8.) Defence Research Establishment Pacific FMO Victoria, B.C. VOS 1B0	2. SECURITY CLASSIFICATION (overall security classification of the document, including special warning terms if applicable)  Unclassified	
3. TITLE (the complete document title as indicated on the title page. Its classification should be indicated by the appropriate abbreviation (S,C,R or U) in parentheses after the title.)  Probability Points for the Kurtosis of a Normal Sample with Known Mean (U)		
4. AUTHORS (Last name, first name, middle initial)  MARANDA, Brian H.		
5. DATE OF PUBLICATION (month and year of publication of document)  November 1994	6a. NO. OF PAGES (total containing information. Include Annexes, Appendices, etc.)  12	6b. NO. OF REFS (total cited in document)  13
7. DESCRIPTIVE NOTES (the category of the document, e.g. technical report, technical note or memorandum. If appropriate, enter the type of report, e.g. interim, progress, summary, annual or final. Give the inclusive dates when a specific reporting period is covered.)  Technical Memorandum		
8. SPONSORING ACTIVITY (the name of the department project office or laboratory sponsoring the research and development. Include the address.)		
9a. PROJECT OR GRANT NO. (if appropriate, the applicable research and development project or grant number under which the document was written. Please specify whether project or grant)  Proj. DRDM-08	9b. CONTRACT NO. (if appropriate, the applicable number under which the document was written)	
10a. ORIGINATOR'S DOCUMENT NUMBER (the official document number by which the document is identified by the originating activity. This number must be unique to this document.)  DREP TM 94-143	10b. OTHER DOCUMENT NOS. (Any other numbers which may be assigned this document either by the originator or by the sponsor)	
11. DOCUMENT AVAILABILITY (any limitations on further dissemination of the document, other than those imposed by security classification)  <input checked="" type="checkbox"/> Unlimited distribution <input type="checkbox"/> Distribution limited to defence departments and defence contractors; further distribution only as approved <input type="checkbox"/> Distribution limited to defence departments and Canadian defence contractors; further distribution only as approved <input type="checkbox"/> Distribution limited to government departments and agencies; further distribution only as approved <input type="checkbox"/> Distribution limited to defence departments; further distribution only as approved <input type="checkbox"/> Other (please specify):		
12. DOCUMENT ANNOUNCEMENT (any limitation to the bibliographic announcement of this document. This will normally correspond to the Document Availability (11). However, where further distribution (beyond the audience specified in 11) is possible, a wider announcement audience may be selected.)  Unlimited		

Unclassified

SECURITY CLASSIFICATION OF FORM

13. ABSTRACT ( a brief and factual summary of the document. It may also appear elsewhere in the body of the document itself. It is highly desirable that the abstract of classified documents be unclassified. Each paragraph of the abstract shall begin with an indication of the security classification of the information in the paragraph (unless the document itself is unclassified) represented as (S), (C), (R), or (U). It is not necessary to include here abstracts in both official languages unless the text is bilingual).

Probability points are computed for the sample kurtosis of independent, identically distributed Gaussian variates when the sample moments are taken about the true mean. The method of computation allows the accurate determination of the probability points even for small tail probabilities, and values are tabulated for probabilities as small as  $10^{-4}$ . Moreover, the results suggest that the probability points tabulated here may also be used when the sample moments are taken about the sample mean.

(See report for French version of the abstract.)

14. KEYWORDS, DESCRIPTORS or IDENTIFIERS (technically meaningful terms or short phrases that characterize a document and could be helpful in cataloguing the document. They should be selected so that no security classification is required. Identifiers, such as equipment model designation, trade name, military project code name, geographic location may also be included. If possible keywords should be selected from a published thesaurus. e.g. Thesaurus of Engineering and Scientific Terms (TEST) and that thesaurus-identified. If it is not possible to select indexing terms which are Unclassified, the classification of each should be indicated as with the title.)

Characteristic Function  
False Alarm  
Gaussian  
Kurtosis  
Normal  
Probability  
Sampling

Unclassified

SECURITY CLASSIFICATION OF FORM

# 149065

NO. OF COPIES NOMBRE DE COPIES	COPY NO. COPIE N°	INFORMATION SCIENTIST'S INITIALS INITIALES DE L'AGENT D'INFORMATION SCIENTIFIQUE
1	1	JL
AQUISITION ROUTE FOURNI PAR	DREP	
DATE	18 Jan 95	
DSIS ACCESSION NO. NUMÉRO DSIS		

DND 1168 (6-87)



**PLEASE RETURN THIS DOCUMENT  
TO THE FOLLOWING ADDRESS:**

DIRECTOR  
SCIENTIFIC INFORMATION SERVICES  
NATIONAL DEFENCE  
HEADQUARTERS  
OTTAWA, ONT. - CANADA K1A 0K2

**PRIÈRE DE RETOURNER CE DOCUMENT  
À L'ADRESSE SUIVANTE:**

DIRECTEUR  
SERVICES D'INFORMATION SCIENTIFIQUES  
QUARTIER GÉNÉRAL  
DE LA DÉFENSE NATIONALE  
OTTAWA, ONT. - CANADA K1A 0K2